

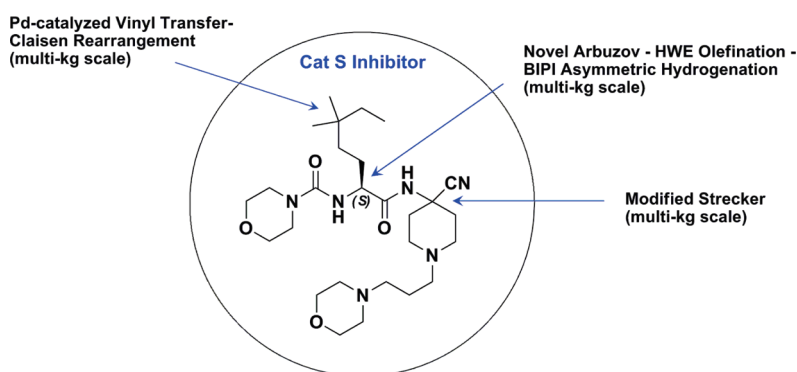
Large-Scale Asymmetric Synthesis of a Cathepsin S Inhibitor

Jon C. Lorenz,^{*,†} Carl A. Busacca,^{*} XuWu Feng, Nelu Grinberg, Nizar Haddad, Joe Johnson, Suresh Kapadia, Heewon Lee, Anjan Saha, Max Sarvestani, Earl M. Spinelli, Rich Varsolona, Xudong Wei, Xingzhong Zeng, and Chris H. Senanayake

Department of Chemical Development, Boehringer-Ingelheim Pharmaceuticals, Inc., 900 Ridgebury Road, Ridgefield, Connecticut 06877

jon.lorenz@boehringer-ingelheim.com

Received November 6, 2009



A potent reversible inhibitor of the cysteine protease cathepsin-S was prepared on large scale using a convergent synthetic route, free of chromatography and cryogenics. Late-stage peptide coupling of a chiral urea acid fragment with a functionalized aminonitrile was employed to prepare the target, using 2-hydroxypyridine as a robust, nonexplosive replacement for HOBT. The two key intermediates were prepared using a modified Strecker reaction for the aminonitrile and a phosphonation–olefination–rhodium-catalyzed asymmetric hydrogenation sequence for the urea. A palladium-catalyzed vinyl transfer coupled with a Claisen reaction was used to produce the aldehyde required for the side chain. Key scale up issues, safety calorimetry, and optimization of all steps for multikilogram production are discussed.

Introduction

Autoimmune diseases such as rheumatoid arthritis (RA) and multiple sclerosis (MS) occur when an immune response is mounted against self-antigens resulting in chronic inflammation and injury to the tissue. The surface bound MHC class II peptide complex engages CD4⁺T cells, which precipitates an immune response. MHC class II heterodimers have been shown to associate intracellularly with a molecule designated invariant chain (Ii). Research suggests that the Ii is selectively proteolyzed by a series of enzymes with the final

step carried out by cathepsin S, a 24 kD cysteine protease from the papain superfamily.¹ Amidonitrile **1** was identified as a potent, selective, and *reversible* inhibitor of cathepsin S.² An efficient, scalable, and safe asymmetric route to kilogram quantities of **1** was required for initial drug development.

Results and Discussion

The retrosynthetic analysis of amidonitrile **1** is shown in Scheme 1. We expected to couple chiral urea acid **2** and aminonitrile **5** to achieve a convergent assembly strategy.³ These advanced intermediates would in turn be derived from an olefination–asymmetric hydrogenation sequence and a Strecker cyanation, respectively.

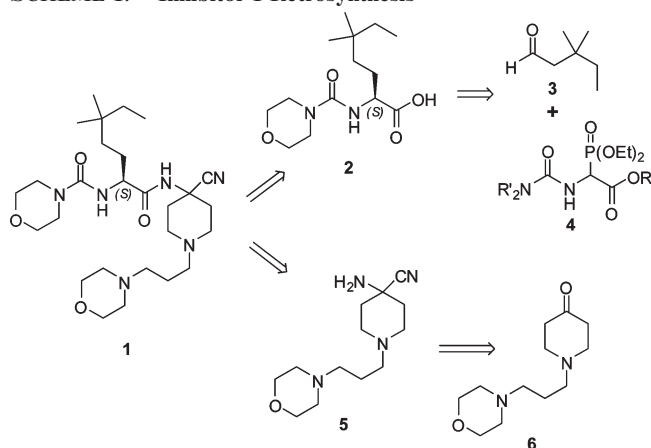
[†]To whom all correspondence should be addressed.

(1) (a) Gupta, S.; Singh, R. K.; Dastidar, S.; Ray, A. *Expert Opin. Ther. Targets* **2008**, *12*, 291–299. (b) Ward, Y. D.; Thomson, D. S.; Frye, L. L.; Cywin, C. L.; Morwick, T.; Emmanuel, M. J.; Zindell, R.; McNeil, D.; Bekkali, Y.; Girardot, M.; Hrapchak, M.; DeTuri, M.; Crane, K.; White, D.; Pav, S.; Wang, Y.; Hao, M.-H.; Grygon, C. A.; Labadia, M. E.; Freeman, D. M.; Davidson, W.; Hopkins, J. L.; Brown, M. L.; Spero, D. M. *J. Med. Chem.* **2002**, *45*, 5471–5482.

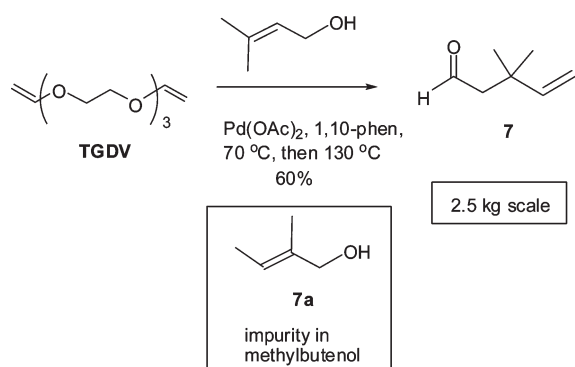
(2) Hickey, E. R.; Liu, W.; Sun, S.; Ward, Y. D.; Young, E. R. R. U.S. Patent CAN 141:243834, **2004**.

(3) For reviews, see: (a) Bertz, S. *Chem. Commun.* **2001**, 2516–2517. (b) Andraos, J. *Org. Process Res. Dev.* **2006**, *10*, 212–240.

SCHEME 1. Inhibitor 1 Retrosynthesis



SCHEME 2. Vinyl Transfer-Claisen



Aldehyde **3** was initially prepared by reduction of the ester precursor with a pyrrolidine-modified Red-Al reagent useful for this type of partial reduction.⁴ The commercial supply of this raw material was capricious, however, and a route which was unaffected by this market condition was needed. We decided instead to prepare the aldehyde by a Claisen rearrangement⁵ of a vinyl ether followed by a trivial olefin hydrogenation. Preparation of these types of vinyl ethers has been achieved with Hg(II),⁶ yet the use of mercury is unacceptable in drug development. We instead used a palladium/phenanthroline catalyst system.⁷

When the vinyl ether exchange step reached equilibrium (easily monitored by ¹H NMR or GC), the catalyst was *deliberately poisoned* with an alkyne to prevent Pd-mediated side reactions, and the temperature was gradually raised first to 120 °C (reflux) and then to 145 °C. The rearrangement was complete in about 3 h. The crude aldehyde was then distilled directly from the reaction mixture (bp ~100 °C/60 mm) and then redistilled through a 60 cm × 2.5 cm vacuum-jacketed column packed with Pro-Pak at atmospheric pressure (130 °C, 24 theoretical plates), furnishing 2.5 kg of pure aldehyde **7** with an overall yield of 60% (Scheme 2).⁸ The isomeric butenol

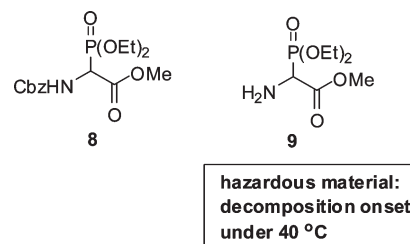


FIGURE 1. Glycine equivalents.

7a was found to be the principal impurity (ca. 1.5%) in commercial 3-methyl-3-buten-1-ol, necessitating the fractional distillation. This was found to be the only point at which the isomeric aldehyde could be removed in the synthetic pathway. As expected, low-pressure hydrogenation of this olefin furnished aldehyde **3** in high yield, although we hoped that this hydrogenation and the expected asymmetric hydrogenation might conceivably be telescoped as well, and this transformation was deferred.

With the aldehyde fragment in hand, our attention turned to the phosphonate partner. Our initial work started from the commercially available Cbz-protected α -phosphonoglycine methyl ester **8**. After hydrogenolysis of the Cbz with Pd/C in alcohol solvent to give **9**, we planned to switch solvent and add morpholine carbonyl chloride to form the required urea. However, process safety calorimetry results readily revealed that although the amino phosphonoester was stable in methanol solution up to 100 °C, the concentrated product was found to have a decomposition onset temperature of under 40 °C. Decomposition energy during the decomposition of **9** was surprisingly high, at 410–460 J/g, which classifies this as an energetic material (Figure 1).

This process safety finding immediately altered our synthetic strategy. We therefore searched for an alternative solvent which would allow hydrogenation followed directly by urea formation without the isolation of hazardous amine **9**. Calorimetry showed a greater solution stability of amine **9** in THF relative to MeOH. After concentration to 20% of its original volume, the THF solution of **9** was still stable up to 100 °C, which was within our acceptable safety margins for initial development work. The hydrogenolysis reaction was carried out in THF with water–wet Pd/C at 100 psig H₂, so that solvent exchange was eliminated. At the conclusion of the reduction, the reaction mixture was filtered through a pad of magnesium sulfate to remove catalyst and water and the filtrate used directly for the subsequent urea formation without any other purification (Scheme 3).

This was achieved by simply charging morpholine carbonyl chloride and *N*-methylmorpholine to the crude solution. Following the urea formation, an aqueous workup was avoided due to the unexpected and significant water solubility of intermediate **10**. Base screening for the HWE (Horner–Wadsworth–Emmons) reaction revealed that 2 equiv of DBU led to good reactivity of phosphonate **10** with aldehyde **7** at 0 °C. However, DBU proved to be a poor base for the previous condensation of **9** with morpholine carbonyl chloride, so two different amine bases were required for this sequence. Diene **11** was isolated as a solid in 150/1 *Z/E* ratio in 60% overall yield from the commercially available Cbz glycine phosphonoester **8**. Although this route supplied material for initial process research, the thermal stability issues

(4) Kanazawa, R.; Tokoroyama, T. *Synthesis* **1976**, 526–257.

(5) For a review, see: Castro, A. M. M. *Chem. Rev.* **2004**, *104*, 2939–3002.

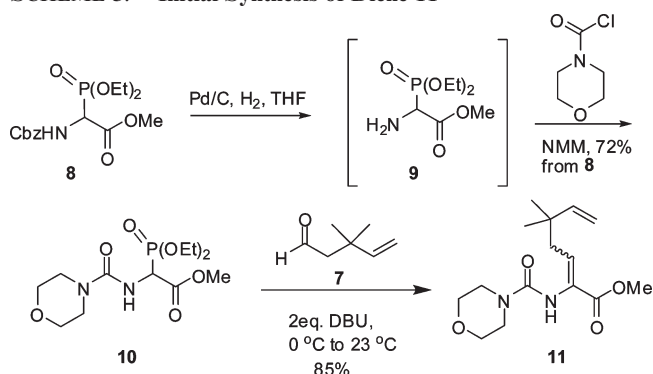
(6) Saucy, G.; Marbet, R. *Helv. Chim. Acta* **1967**, *50*, 2091–2095.

(7) (a) McKeon, J. E.; Fitton, P.; Griswold, A. A. *Tetrahedron* **1972**, *28*, 227–232. (b) McKeon, J. E.; Fitton, P. *Tetrahedron* **1972**, *28*, 233–238.

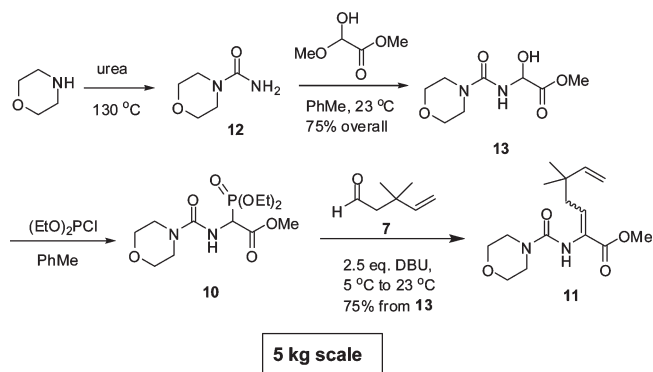
(8) (a) Wei, X.; Lorenz, J. C.; Kapadia, S.; Saha, A.; Haddad, N.; Busacca, C. A.; Senanayake, C. H. *J. Org. Chem.* **2007**, *72*, 4250–4253.

(b) See the Supporting Information.

SCHEME 3. Initial Synthesis of Diene 11



SCHEME 4. Kilogram-Scale Synthesis of Diene 11

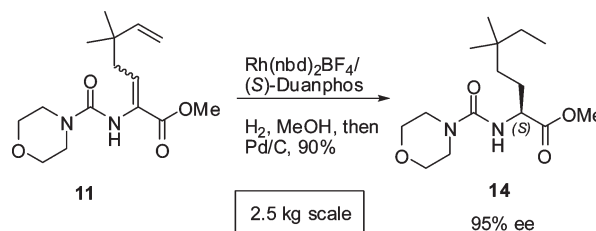


with amine **9** required us to develop a safer process to make this key diene.

As shown in Scheme 4, our alternative route to the dienyl ester began with the reaction of morpholine and urea in xylenes at 130 °C for 8 h followed by cooling to 22 °C giving **12** as a crystalline solid which was easily isolated by filtration. Urea **12** was then condensed with inexpensive methyl glyoxylate hemiacetal in toluene at 22 °C which furnished hydroxyurea ester **13** as a precipitate which could again be readily isolated by filtration. We observed some variability in isolated yield for this transformation and thus utilized in situ IR to study it in more detail. We were able to observe that after the starting material went into solution, the product slowly started to precipitate but then redissolved. The solubility of the product was caused by the methanol liberated during the course of the reaction, so we therefore instituted an in-process removal of methanol by distillation under 50 °C to ensure full precipitation of the product. In this way, hydroxyurea **13** could be isolated in 75% overall yield.

Conversion of **13** to the phosphonate was first attempted via a traditional Michaelis–Arbuzov-type reaction⁹ where the alcohol was initially converted to a chloride with thionyl chloride at –15 °C, followed by addition of triethyl phosphite to form the phosphonate **10**. However, the chloro intermediate was found to be unstable and reacted readily with the starting material to produce dimeric impurities. An alternative preparation of **10** was therefore developed using

SCHEME 5. Rh/(S)-DuanPhos Hydrogenation



chloro diethylphosphite in a modified Michaelis–Arbuzov reaction. Here the hydroxyl group nucleophilically attacks the chlorophosphite, followed by what we presume must be a facile phosphite-to-phosphonate rearrangement, as the product was spectroscopically identical to **10** prepared via the standard Michaelis–Arbuzov process. This may well be a novel transformation, and the mechanism of the rearrangement is not certain. This could simply involve a thermal process to the more thermodynamically stable phosphonate, or possibly an initial elimination to an acylimine followed by addition of a phosphorus nucleophile, such as diethylphosphite, generated in situ. This sequence nevertheless allows for an extremely convenient and economical one-pot conversion of hydroxyurea **13** to key phosphonate **10**, without having to resort to low-temperature reaction conditions and utilizing an inexpensive chlorophosphite readily available in multikilogram quantities. The product was formed in 75% overall yield, on a 5 kg scale, from hydroxyurea **13** as a > 30:1 *Z/E* mixture. Further studies on this reaction will be published in due course.

With a stable and scalable route to diene **11** in hand, we turned our attention to the critical asymmetric hydrogenation. A rapid screen of commercial homogeneous hydrogenation conditions showed that the prochiral olefin could be hydrogenated with high enantioselectivity using Rh(I) with either TangPhos or DuanPhos, developed by Zhang.¹⁰ The enantiomer of TangPhos needed for target **1** is prepared using chiral stationary phase chromatography, however. We therefore employed DuanPhos, which is prepared via classical resolution, for our initial hydrogenation scale-up (Scheme 5).

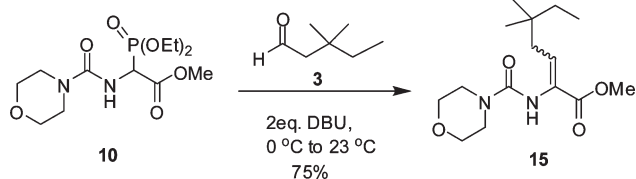
Rh(I)-(S)-DuanPhos was used to first reduce the functionalized olefin, and Pd/C was then charged to reduce the terminal olefin. The product was produced with 95% ee at 1% catalyst loading, and we were able to prepare over 2.5 kg of material using this protocol. A screen of conditions for removing the residual Rh and Pd from **14** was then initiated. Key findings were that metal removal was much more efficient at elevated temperatures (50–60 °C) and that polar solvents like methanol were superior to nonpolar ones. Of numerous scavengers examined, Darco KB activated carbon was observed to be the most efficient at metal removal. After the hydrogenation, we thus performed a hot slurry of ester **14** in methanol with Darco KB and removed both metals to < 10 ppm as determined by ICPMS.

During this hydrogenation campaign, we found that careful cleaning of the hydrogenation reactor between runs had to be carried out to avoid residual Pd which would lead to a “background” racemic hydrogenation pathway in the

(9) For a review, see: (a) Bhattacharya, A. K.; Thyagarajan, G. *Chem. Rev.* **1981**, *81*, 415–430. See also: (b) Quin, L. *A Guide to Organophosphorus Chemistry*; Wiley: New York, 2000; pp 141–152.

(10) (a) Tang, W.; Zhang, X. *Angew. Chem., Int. Ed.* **2002**, *41*, 1612–1614. (b) Liu, D.; Zhang, X. *Eur. J. Org. Chem.* **2005**, *4*, 646–649.

SCHEME 6. Alternate HWE Olefination



Rh/DuanPhos reduction. The decision was thus made to hydrogenate the terminal olefin *prior* to the HWE olefination. The type of Pd/C used for the hydrogenation of aldehyde **7** to aldehyde **3** had a large effect on the rate of the reaction with 5% Pd/C–50% H₂O Degussa-type E1002E/W giving the best results. Since the aldehyde was an oil, we were able to perform the hydrogenation *without solvent*, achieving maximum volume efficiency. At 0.25 wt % catalyst charge, the reaction was rapid and exothermic so that cooling had to be applied to maintain the internal temperature below 35 °C.

Saturated aldehyde **3** could be isolated after simple filtration to remove the catalyst and then used in the HWE reaction without further purification. This strategy also moved the use of Pd to an earlier point in the synthesis so that no special measures were required to remove this metal from the final compound. As expected, the saturated aldehyde performed well in the olefination reaction giving ester **15** in ~75% yield from phosphonate **10** (Scheme 6).

We next focused on developing in-house ligands to carry out this asymmetric hydrogenation in order to lower the overall cost of drug development for this program. We have recently reported a novel family of chiral phosphinoimidazolines, the BIPI ligands, and their application to various catalytic asymmetric transformations.¹¹ At the time of this cathepsin S project, however, we had not yet attempted to apply these ligands in asymmetric hydrogenations. Screening a diverse set of these ligands from our library revealed that only BIPI ligands with dialkyl substitution on phosphorus and an acyl substituent on the nitrogen gave good turnover when complexed in situ with a cationic rhodium(I) precatalyst for hydrogenation. In addition, we found that the phosphorus substituents had to possess both α -substitution and β -branching to achieve both turnover and selectivity. The nature of the aryl group on the imidazoline (derived from the chiral diamine) was also important, and the unsubstituted system proved to be optimum. BIPI 69 (Figure 2) furnished the product in 95% ee, and this was our optimum ligand throughout much of the process development. In all cases, the (*S,S*)-ligand series was found to provide the desired (*S*) stereochemistry in the hydrogenation product.

We were particularly interested in determining the optimum ligand/catalyst ratio. Contrary to our intuition, a slight excess of rhodium relative to ligand (1.5:1) actually provided the highest selectivities. We performed the reduction of diene

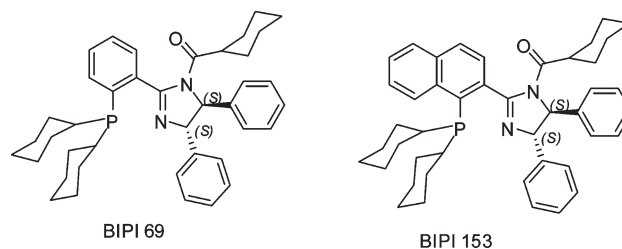


FIGURE 2. BIPI ligands.

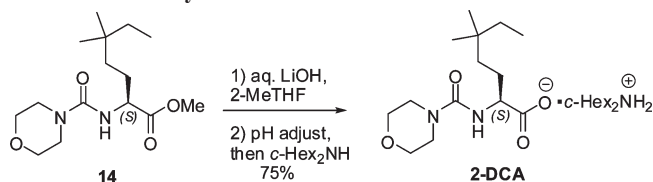
15 with BIPI 69, increasing the batch size in stages. As we prepared for larger scale hydrogenations, we wanted to ensure that we had developed a robust method to set the required stereocenter. Initial success with BIPI 69 led us to test the oxidized ligand (BIPI 69 phosphine oxide) with Rh(nbd)₂BF₄ to see if it would lead to unselective reduction. Although the analogous rhodium complex could be formed (as determined by a diminished, though readily observable, ³¹P–¹⁰³Rh coupling in the ³¹P NMR), only trace amounts of product were observed in the hydrogenation, giving us confidence that small amounts of oxygen from incomplete reactor inertion would not compromise the enantioselectivity. When catalyst loading was reduced to 0.2 mol %, some batch-to-batch variability was observed.^{12a} When a sample of one of the larger batches was dissolved in MeTHF, an insoluble white solid was observed, raising concerns that there could be some salts carried forward from the olefination step which could then alter the ligand sphere around rhodium. The culprit was found to be a chloride ion-containing salt, inadvertently introduced following the use of dilute HCl and/or brine in the workup of intermediate **11**. The workup was thus changed to remove all chloride, using aq H₂SO₄ in place of HCl and omitting the brine wash. The deleterious effects of chloride in olefin asymmetric hydrogenations have been observed previously.^{12b} We ultimately carried out this hydrogenation on 2 kg scale and were able to drop the catalyst load to only 0.07 mol % (0.0007 equiv, 0.00125 g of Rh(nbd)₂BF₄/g substrate), lower than our initial target catalyst load. BIPI 153, with the naphthyl core, was subsequently prepared and observed to give near-perfect enantioselectivity for this hydrogenation.^{11a,b}

The crude hydrogenation mixture was treated with Darco KB at 60 °C as described previously, followed by a Celite filtration. The filtered MeOH solution of ester **14** was concentrated to ~50 wt % by distillation, then MeTHF was added followed by 1.6 M LiOH, to effect saponification. When the solution of **2** was adjusted to ~20 wt % in MeTHF, small amounts of the racemate were observed to precipitate after several hours aging at ~22 °C. In this way, solutions of **2** with diminished optical purity could be significantly upgraded, to ~97–99% ee, simply by filtration of the racemate from dry ethereal solvents. The solvent was next switched to *i*-PrOAc by azeotropic distillation and the concentration adjusted to 20 wt % **2**. The product chiral acid **2** (Scheme 7) is an oil with a melting point below –40 °C, and exhaustive attempts to crystallize the free acid did not

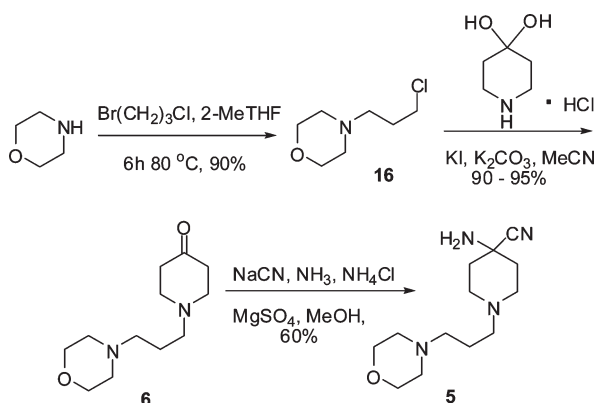
(11) (a) Busacca, C. A.; Lorenz, J. C. U.S. Patent CAN 149:10123, 2007. (b) Busacca, C. A.; Lorenz, J. C.; Grinberg, N.; Haddad, N.; Lee, H.; Li, Z.; Liang, M.; Reeves, D.; Saha, A.; Varsolona, R.; Senanayake, C. H. *Org. Lett.* 2008, 10, 341–344. (c) Busacca, C. A.; Grossbach, D.; Campbell, S.; Dong, Y.; Eriksson, M.; Harris, R. E.; James-Jones, P.; Kim, J.-Y.; Lorenz, J. C.; McKellop, K. B.; O'Brien, E. M.; Qiu, F.; Simpson, R. D.; Smith, L.; So, R.; Spinelli, E. M.; Vitous, J.; Zavattaro, C. *J. Org. Chem.* 2004, 69, 5187–5195. (d) Busacca, C. A.; Grossbach, D.; So, R.; O'Brien, E. M.; Spinelli, E. M. *Org. Lett.* 2003, 5, 595–598. (e) Busacca, C. A. U.S. Patent CAN 134:207967, 2001.

(12) (a) For a review on catalyst inhibition, see: Heller, D.; de Vries, A. H. M.; de Vries, J. G. In *Handbook of Homogeneous Hydrogenation*; de Vries, J. G., Elsevier, C. J., Eds.; Wiley-VCH:Weinheim, 2007; pp 1483–1516. (b) Cobley, C. J.; Lennon, I. C.; Praquin, C.; Zanolli-Gerosa, A.; Appell, R. B.; Goralski, C. T.; Sutterer, A. C. *Org. Process Res. Dev.* 2003, 7, 407–411.

SCHEME 7. Crystalline Salt 2·DCA



SCHEME 8. Synthesis of Aminonitrile 5



provide a solid. Salt screening, however, identified dicyclohexylamine as a good amine for robust crystallization of the acid salt. In practice, a portion of the dicyclohexylamine was added at ~ 40 °C, seeds were charged, and then the remaining amine added to form the 2·DCA salt. This crystalline salt was then collected by filtration, rinsed with heptane, and dried to give the first final intermediate in 75% yield from ester **14**.

With preparation of the key chiral acid accomplished, we turned our attention to the aminonitrile **5**. The precursor ketone **6** was prepared via straightforward base-free alkylation of morpholine with bromochloropropane followed by addition of piperidone, as shown in Scheme 8.

The very water-soluble morpholine piperidone **6** was prepared starting from morpholine to yield **16** which was reacted with inexpensive piperidone hydrochloride monohydrate. This two-step procedure provided high purity ketone for the Strecker reaction utilizing GC for all in-process testing. Attempted use of the dihydrochloride salt of **6** in the Strecker reaction gave the dimethyl ketal, causing severe complications.

Performing a Strecker aminonitrile synthesis on multi-kilogram scale requires careful attention to safety, due to large quantities of cyanide used. We opted to work with a third party manufacturer with experience in this area. The Strecker was readily carried out using a buffered ammonia/ammonium chloride system with in situ drying agent to furnish the target aminonitrile **5** in 60% overall yield. We performed a head space analysis of this packaged nitrile and discovered that low levels of HCN, ca. 2 ppm, were produced on standing. This finding complicated many aspects of the project. Trans-Atlantic shipping of any material which generates HCN, a severe poison, will be difficult, since most carriers are not licensed to transport such compounds. This in fact required that we move production of this key intermediate to the United States, where surface shipping was again possible. The HCN was presumably formed via a

retro-Strecker reaction. This is a known issue with aminonitriles¹³ and is usually overcome by forming a salt of the amine. In the current case, however, protonation of the primary amine is very difficult since there are two more basic amines in the molecule. The pK_a 's of these other basic sites were determined experimentally to be 6.0 and 7.4. In attempts to stabilize this species, tartrates, sulfates, and hydrochlorides of **5** were prepared, and the tartrate was found to be the least hygroscopic. When the bis-tartrate salt was held at 100 °C for 16 h in a DSC (Differential Scanning Calorimetry), however, significant decomposition to ketone **6** was observed, as monitored by LCMS of the sample, suggesting that HCN was again being evolved. Attempts to protect the aminonitrile with an electron-withdrawing group, preventing the retro-Strecker, were also unsuccessful. This led us to develop a crystallization strategy for the aminonitrile free base. Initial success was achieved using isopropyl acetate (IPAc) as crystallization solvent, yet better crystal growth (following seeding) was observed from an ethyl acetate (pro-solvent)/heptane (antisolvent) system due to the greater solubility of **5** in EtOAc. At scale the key process parameter was found to be the concentration of the aminonitrile/EtOAc solution. A concentration of 33 wt % proved to be optimum, with more concentrated systems causing **5** to oil out.

We then turned to the endgame strategy for inhibitor **1**. Early investigation into this step showed that mixed anhydrides formed from chloroformates and acid chlorides were not acceptable. We initially coupled aminonitrile **5** with acid **2** using a standard EDC/HOBT protocol, in MeTHF or MeTHF/DMF mixtures, to generate **1** in >90% isolated yield. This approach allowed us to prepare the initial kilogram quantities of the target. However, HOBT and related benzotriazoles are classified as explosives in Europe.¹⁴ We therefore wanted to replace HOBT, if possible, prior to internal technology transfer. A significant screening program for this critical peptide coupling was then initiated, and the results were collected in Table 1.

We attempted initially to use the dicyclohexylamine salt of acid **2** (2·DCA) in the peptide coupling. Although the couplings with EDC were successful, the dicyclohexyl amine remained in the organic layer and inhibited the final crystallization. We ultimately found that the use of 0.5 M H_2SO_4 and MeTHF gave two clear phases following the salt break. The solution of acid **2** thus obtained was dried by azeotropic distillation prior to the peptide coupling. This procedure was then employed for all the screening reactions.

Figure 3 shows all of the weak acids and coupling reagents examined for the peptide coupling. The use of the coupling reagents CDI and DCC with weak acid A gave poor conversion (Table 1, entries 2 and 3), and the latter also led to significant racemization. Therefore, we focused our efforts on EDC. EDC in the absence of HOBT (Table 1, entry 4) also furnished the product with low optical purity. *N*-Hydroxysuccinimide was observed to be a poor choice of weak acid (Table 1, entry 7), likely due to its lower acid strength. Hydroxybenzotriazinone **D** was found to be a good weak acid under a variety of conditions (Table 1, entries 9–17), yet

(13) (a) Rossi, J.-C.; Marull, M.; Boiteau, L.; Taillades, J. *Eur. J. Org. Chem.* **2007**, 662–668. (b) Pascal, R.; Taillades, J.; Commeyras, A. *Tetrahedron* **1978**, *34*, 2275–2281.

(14) Weisenburger, G. A.; Vogt, P. F. *Org. Process Res. Dev.* **2006**, *10*, 1246.

TABLE 1. Peptide Coupling of 5 and 2

no.	solvent	reagent	weak acid	conv ^a (%)	ee ^b (%)
1	THF	EDC	A	90	91
2	THF	CDI	A	20	ND
3	MeCN	DCC	A	81	82
4	MeCN	EDC	None	96	56
5	MeCN	EDC	B	76	98
6	THF	EDC	B	77	97
7	THF	EDC	C	36	ND
8	THF	EDC ^f	B	73	99
9	MTHF ^c	EDC	D	90	83
10	THF ^c	EDC	D	90	99
11	MTHF ^c	EDC	D	93	99
12	THF ^d	EDC	D	90	99
13	MTHF ^e	EDC	D	93	99
14	THF ^e	EDC	D	91	99
15	DMF	EDC	D	88	98
16	MTHF ^c	EDC	D	94	99
17	MTHF ^c	EDC	D	97	86
18	MTHF ^c	EDC	A	90	99
19	MTHF ^c	EDC	B	93	98
20	MTHF ^c	EDC	E	93	96
21	MTHF ^c	EDC	F	7	ND
22	MTHF ^c	EDC	G	95	98
23	MTHF ^c	EDC	H	95	98
24	MTHF ^c	EDC	I	88	97
25	MTHF ^c	EDC	J	77	98
26	MTHF ^c	EDC	K	93	96
27	MTHF ^c	EDC	L	81	97

^a% by HPLC. ^b% by chiral HPLC. ^cWith DMF. ^dWith DMAc. ^eWith NMP. ^fDIEA added.

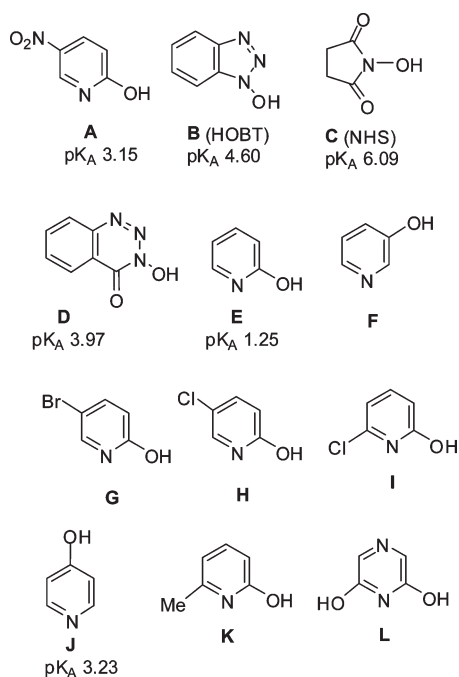
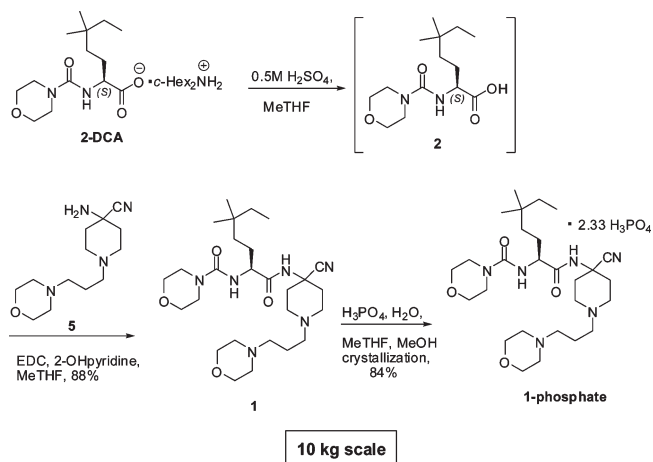


FIGURE 3. Weak acids screened.

its higher cost and potential for being an energetic and shock sensitive material like HOBT induced us to search further. We next screened several substituted pyridines as potential weak acids. All of the hydroxypyridines screened (E–K) were stable up to at least 320 °C as determined by DSC. In addition, they all provided the adduct with essentially no

SCHEME 9. Final Assembly of Inhibitor 1



racemization (nos. 20–27), though the same failed to give full conversion. We were ultimately able to select 2-hydroxypyridine from this group as a robust replacement for HOBT¹⁵ in MeTHF. This solvent choice also allowed us to eliminate DMF from the reaction, which had been observed at levels up to ~2000 ppm in several early batches of 1. This EDC/2-hydroxypyridine process was then successfully demonstrated on an 11 kg scale, giving crude 1 in 88% isolated yield. This coupling and completion of the synthesis of cathepsin S inhibitor 1 are shown in Scheme 9.

Completion of the drug substance campaign then required only the formation of a pharmaceutically acceptable salt form. Solid-state screening identified the phosphate salt as having the desired properties. After the peptide coupling, the crude 1 in a solution of wet MeTHF was concentrated to about 50 wt % by distillation and the concentrated solution then diluted to 25 wt % with methanol and clarified by filtration. A solution of H₃PO₄ was then added to achieve a target pH of 2.9–3.1. The KF (Karl Fischer water titration) of the solution was adjusted to 11.4% since water was found to allow the crystals to grow instead of precipitating out of solution. The mixture was then warmed to ~60 °C to obtain a clear solution. Cooling of the resultant solution to 57 °C and seeding with the desired polymorph induced batch crystallization. The resultant thin slurry was then aged at ~55 °C for 60 min to develop the seed bed, followed by a slow cooling ramp to ambient temperature to grow plate-shaped crystals. The solid was then collected by vacuum filtration under a nitrogen blanket. This crystallization was found to upgrade the optical purity to ~99% ee (when BIPI 69 was used for the asymmetric hydrogenation) and also to increase the chemical purity substantially. A reproducible nonstoichiometric 2.33 phosphate was formed in this way. This phosphate salt crystallization protocol was ultimately successfully demonstrated on more than 10 kg scale.¹⁶

(15) (a) Dunn, P. J.; Hoffmann, W.; Kang, Y.; Mitchell, J. C.; Snowden, M. J. *Org. Process Res. Dev.* **2005**, *9*, 956–961. (b) El-Faham, A.; Albericio, F. *Eur. J. Org. Chem.* **2009**, *10*, 1499–1501. (c) Bright, R.; Dale, D. J.; Dunn, P. J.; Hussain, F.; Kang, Y.; Mason, C.; Mitchell, J. C.; Snowden, M. J. *Org. Process Res. Dev.* **2004**, *8*, 1054–1058. (d) Dutta, A. S.; Morley, J. S. *J. Chem. Soc. C* **1971**, 2896–2901.

(16) Busacca, C. A.; Haddad, N.; Kapadia, S. R.; Smith Keenan, L.; Lorenz, J. C.; Senanayake, C. H.; Wei, X. U.S. Patent CAN 142:464024, **2007**.

In summary, we have developed a robust, economic, and scalable asymmetric synthesis of a potent cathepsin S inhibitor. New technologies for Claisen rearrangement, olefination, and asymmetric hydrogenation were developed in-house in order to achieve this goal. Significant research on weak acid additives for the critical peptide coupling identified 2-hydroxypyridine as an excellent replacement for hazardous HOBt. All synthetic transformations were carried

out on multikilogram scale, without chromatography or cryogenics, in a highly convergent asymmetric process.

Supporting Information Available: Experimental procedures, compound characterization, calorimetry data for **9**, and ^1H and ^{13}C NMR spectra for all compounds. This material is available free of charge via the Internet at <http://pubs.acs.org>.